Simovski, Constantin R.

Circuit theory of metal-enhanced fluorescence

Published in:
Photonics and Nanostructures - Fundamentals and Applications

DOI:
10.1016/j.photonics.2019.100712

Published: 01/09/2019

Document Version
Peer-reviewed accepted author manuscript, also known as Final accepted manuscript or Post-print

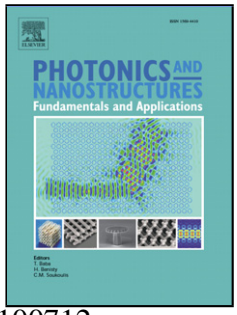

Title: Circuit theory of metal-enhanced fluorescence

Author: Constantin R. Simovski

PII: S1569-4410(19)30054-9
DOI: https://doi.org/doi:10.1016/j.photonics.2019.100712
Reference: PNFA 100712

To appear in: *Photonics and Nanostructures – Fundamentals and Applications*

Received date: 18 February 2019
Revised date: 17 May 2019
Accepted date: 26 May 2019

Please cite this article as: Constantin R. Simovski, Circuit theory of metal-enhanced fluorescence, *<![CDATA[Photonics and Nanostructures - Fundamentals and Applications]]>* (2019), https://doi.org/10.1016/j.photonics.2019.100712

Circuit theory of metal-enhanced fluorescence

Constantin R. Simovski[a,b]

[a] *Aalto University, School of Electrical Engineering, Department of Electronics and NanoEngineering, P.O. Box 15500, 00076 Aalto, Finland*

[b] *ITMO University, Kronverkski pr. 49, 197101, St. Petersburg, Russia*

Abstract

Metal-enhanced fluorescence (MEF) comprises several linear phenomena which can be successfully described either by a classical theory or by a quantum one. Usually different phenomena are described by different classical models. Recently, an analytical model for a metal nanoantenna coupled to a quantum emitter was suggested that grants an approximate solution covering all basic linear phenomena observed in MEF from the Purcell effect to the fluorescent quenching. In this paper, the further development of this model is presented in terms of the equivalent circuits. The circuit model allows us to express the non-radiative Purcell factor of a nanoantenna through the previously evaluated radiative Purcell factor, to find the threshold of the fluorescence quenching and to determine the conditions when a fluorescent nanostructure transforms into a surface-plasmon laser (spaser).

Keywords: Metal-enhanced fluorescence; quantum emitter; nanoantenna; Purcell factor; Rabi oscillations; fluorescence quenching; resonant circuit; mutual impedance; radiative resistance; electromotive force; negative resistance; increment; spaser

1. Introduction

Fluorescent labels and tags are widely used in optical nanosensing and nanoimaging, especially in biological applications [1]. Fluorescence of the dye molecules (rhodamine, rhodanide, etc.) and semiconductor nanocrystals (quantum dots) offers several important possibilities to the nanosensing and nanoimaging, such as detection of very small analytes and dynamic tracking of the cell movement [2, 3, 4, 5]. The enhancement of the fluorescence drastically improving these applications is achieved by placing a quantum emitter (QE) in the vicinity of a plasmonic nanoatenna (NA) so that these two nanoobjects are coupled by near fields. Basically, the enhancement of the emission is granted by a localized surface plasmon to which the fluorescent power is transferred. This plasmon is usually radiative and its radiation is more efficient than that of a single QE. Therefore, the presence of the NA allows the QE to emit the photon faster. This decay rate enhancement allows a single molecule in the continuous wave regime to collect more power from the pumping radiation and the fluorescence saturation threshold grows. For an ensemble of molecules the enhancement of the decay rate implies higher fluorescence for the same pumping level because the molecules capture the photons more frequently.

Plasmons can be excited not only in metal nanoparticles, and not all metals are plasmonic in the optical range. The term *plasmon-enhanced fluorescence* would be more adequate to describe this general phenomenon [6, 7, 8, 9, 10]. However, we will use the term *metal-enhanced fluorescence*, in compliance with the majority of corresponding papers [11, 12, 13, 14] and books, such as [15].

In conventional MEF techniques fluorescent molecules attach to a dielectric shell of a core-shell plasmonic nanoparticle in a colloidal suspension [11, 13, 14]. These molecules form an effective shell as it is shown in the inset of Fig. 1. The plasmons induced by these molecules are excited in the metal core if the fluorescence spectral line overlaps on the frequency axis with the range of the plasmon resonance. The maximal enhancement corresponds to the case when the frequency of the optical transition ω_0 exactly coincides with that of the plasmon resonance. In the present conceptual paper we will consider the latter case (the impact of detuning deserves a separate study).

In fact, the enhancement of the fluorescence in this technique holds only for radially polarized quantum sources as it is shown in Fig. 1(a). In this case the dipole moment $\mathbf{d}_1$ of a molecule induces the resonant dipole $\mathbf{d}_2$ (and perhaps, a set of high-order multipoles) in the NA so that $\mathbf{d}_2$ is parallel to $\mathbf{d}_1$.

For these molecules the near-field dipole coupling can be optimized so that $|\mathbf{d}_2(\omega)| \gg |\mathbf{d}_1(\omega)|$ within the fluorescence band and the total dipole moment of the dimer at the frequency of the optical transition $\mathbf{d}^{\rm tot}(\omega_0)$ has the absolute value much higher than $|\mathbf{d}_1(\omega_0)| \equiv d_1(\omega_0)$. This enhancement demands the proper choice of the dielec-

[☆] The article belongs to the special section Metamaterials.

Email address: konstantin.simovski@aalto.fi (Constantin R. Simovski)

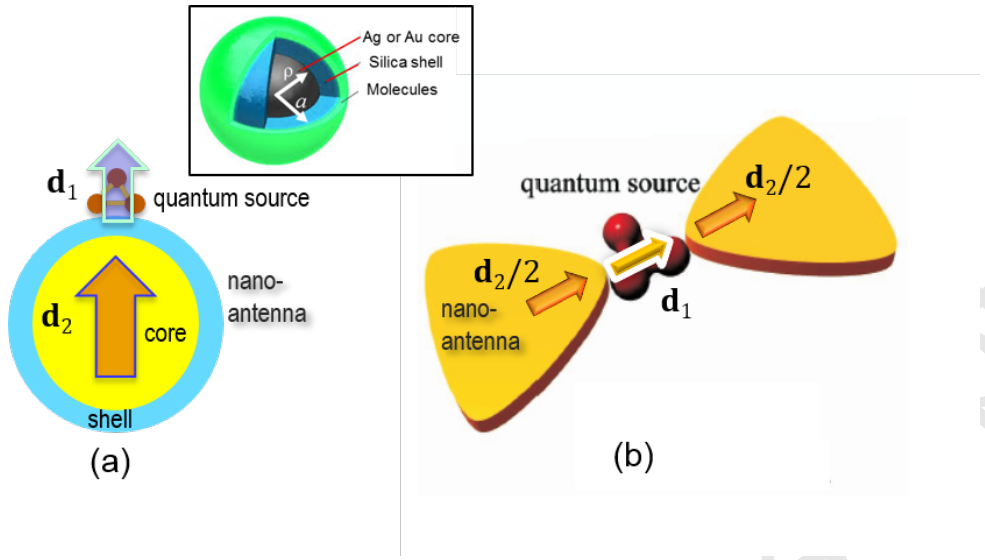

Figure 1: Particular cases of MEF: (a) – a core-shell plasmonic nanoantenna where the dipole moment d_2 is excited by a radially polarized quantum source (dipole moment d_1, (b) – a bow-tie plasmonic NA centered by a quantum source. On the inset a sketch of a core-shell NA with a plasmonic core and a dielectric shell is shown, whereas the fluorescent molecules form an outer shell.

tric shell thicknesses and is referred as the Purcell effect [1, 7, 8, 9, 12, 16, 17]. Usually, the Purcell effect is defined as the decay rate increase granted to a QE by a resonant scatterer [16]. Recently, the concept of the Purcell effect was generalized as the decay rate increase granted to an emitter by any environment different from the usual ambient [18, 19]). In the steady (or continuous-wave) regime, the increase of the dipole moment implies the quadratic increase of the radiated power $P_{\rm rad}$. Since the unit fluorescence event is emission of a photon with the energy $\hbar\omega_0$, the enhancement of $P_{\rm rad}$ evidently grants the increase of the decay rate (decrease of the lifetime of the excited state). The radiative increase of the decay rate is called the radiative Purcell factor $F^P_{\rm rad}$ and the Purcell effect implies that the decay rate increases mainly due to the increase of the radiated power.

Using the commonly known formula for the time-harmonic dipole radiated power, the radiative decay rate $\gamma_{\rm rad}$ and radiative Purcell factor in the case of the Purcell effect are estimated in [18, 19] as follows:

$$\gamma_{\rm rad} = \frac{(\omega_0^4 |d^{\rm tot}(\omega_0)|^2/3\pi\varepsilon_a c^3)}{\hbar\omega_0}, \quad F^P_{\rm rad}(\omega_0) = \left|\frac{d^{\rm tot}(\omega_0)}{d_1(\omega_0)}\right|^2 \gg 1. \tag{1}$$

As to molecules polarized tangentially to the surface of the shell, their near-field coupling with the NA is destructive and results in $F^P_{\rm rad} < 1$ [7, 8, 9, 13]. If the same dipole moment $\mathbf{d}_1$ as in Fig.1(a) is located in the equatorial area of the spherical surface the induced dipole $\mathbf{d}_2$ will be antiparallel. Therefore, we may neglect the tangentially polarized molecules, and consider only a radially polarized QE multiplying the power of its fluorescence in presence of the NA by the number N of molecules coupled with the given spherical NA (green color in the inset of Fig. 1) and by the statistical percentage 1/3 of the radially polarized ones. Really, the fluorescence of different molecules in conventional MEF schemes is not coherent, and one can neglect the electromagnetic interaction between the molecules of the array coupled to a given NA. Therefore, having in mind the factor $N/3$, it is enough to calculate the Purcell factor for a dimer formed by a reference emitter (1) and NA (2) shown in Fig. 1(a).

It is worth to note, that $F^P_{\rm rad}$ is higher when the shell of the core-shell NA is plasmonic and the core is dielectric [7, 10]. Since such plasmon resonances hold in the near infrared, the fluorescence to be enhanced also should occur in the near-infrared range. In this case, the self-assembly of the fluorescent molecules around the shell is still possible – molecules attach to an intermediate monolayer of non-fluorescent ligand molecules. The ligand molecules naturally cover the metal surfaces [7, 10, 15]. This technique of the fluorescence enhancement is advantageous because the metal shell is tiny and the dissipation in it is lower than in the case when the plasmon is excited in a more substantial core. The lower dissipation implies the lower dissipative Purcell factor $F^P_{\rm dis}$ that also grants the decay rate enhancement. However, this enhancement is not due to the power radiated by the dimer but due to the power absorbed in the NA. Power emitted by the QE during a unit event comprises two additive components – power absorbed in the NA and power transferred to the ambient, Therefore, the total Purcell factor $F^P_{\rm tot}$ (the increase of the decay rate granted to the QE by the NA) is the sum of $F^P_{\rm rad}$ and $F^P_{\rm dis}$. For metal nanoshells $F^P_{\rm rad}$ is noticeably higher than $F^P_{\rm dis}$, and for metal nanocores the situation is opposite.

Further enhancement of $F^P_{\rm rad}$ is granted by more elaborated NAs, such as plasmonic bow-tie, plasmonic nanorod, plasmonic dual patch and some others (see e.g. in [20, 21, 22]). Fig. 1(b) illustrates the experiment in which a sin-

gle QE centered in the gap of a bow-tie NA was detected [20]. It is possible for QEs polarized axially, since for the transverse polarization the coupling is not constructive.

Apart from the resonance enhancement (referred to as the Purcell effect) in MEF, there are several phenomena owing to linear electrodynamics but resulting from the strong coupling between the QE and NA. If the coupling is strong enough for the modification of the fluorescence spectrum, the fluorescence gain decreases. Maximal values of the radiative Purcell factor (exceeding one hundred) can be achieved namely in the case of the rather weak near-field coupling. Of course, in order to obtain $F^P_{\rm rad} \gg 1$ the coupling should be sufficient. However, its electromagnetic weakness means that the action of the NA to the optical transition in the QE is negligibly low and the dipole moment $\mathbf{d}_1(\omega_0)$ is preserved. Below we will mathematically formulate the criterion of the electromagnetic weakness of the coupling in a dimer.

Imagine that we gradually reduce the dielectric shell of a plasmonic core shown in Fig. 1(a) or shrink the gap of a bow-tie antenna depicted in Fig. 1(b). Then we gradually transit from the regime of the weak coupling (Purcell effect) to the regime of the strong coupling, when the fluorescence spectrum modifies. In the weak-coupling regime the QE is still a a two-level quantum system. Being strongly coupled to a NA it becomes an emitter with two excited states. The energy exchange commences between these states called the Rabi oscillations starts [17, 22, 23, 24]. These oscillations can be either radiative or non-radiative. In the latter case, the fluorescence is suppressed (quenched) by the NA [25, 26, 27]. If the emissivity of the QE is high enough in the regime of non-radiative Rabi oscillations the power of the emitted photons transferred to the NA may exceed the power returned by the NA back to the QE. Then the amplitude of the localized surface plasmon excited in a plasmonic NA starts to grow. Though this growth is not a subject of the present paper, let us note that this growth results in both non-linearity of the oscillations and in the rise of the coherent (stimulated) oscillation competing with the non-coherent emission. Such a nanostructure was suggested in [28] and called *spaser* that means surface plasmon laser. In this analogue of a laser, the role of the induced radiation is played by the stimulated plasmon and the positive feedback necessary for generation is granted by the power exchange in the dimer [29, 30].

Nowadays, in the scientific community there is an insight that the Purcell effect in a quantum dimer is a classical phenomenon. It can be precisely described via the Green function, however, quite often can be adequately modelled as the effect of the weak dipole coupling [19]. The radiative Purcell factor is an increase of the radiative resistance of a QE granted by the presence of the NA, and the dissipative one is the increase of the dissipative resistance due to the optical loss inherent to the plasmon resonance. This is now a commonly adopted opinion. However, in what concerns the strong near-field coupling there is no such commonly adopted opinion, and different authors promote different points of view. The goal of the present paper is to explain that all linear effects observed in MEF, from the Purcell effect in a conventional MEF scheme to the transient regime of a spaser, can be described classically. Moreover, for simple nanosystems, as those sketched in Fig. 1, this classical description is possible in terms of time-harmonic dipole-dipole interaction. The obtained closed-form solution offers an interpretation of all these effects via equivalent *RLC*-circuits.

2. Circuit theory of a fluorescent dimer

2.1. Fluorescence of a dipole dimer

If the coupling is not weak and not very strong the spectral line of the fluorescence experiences a red shift whereas the spectral dependence of $|d^{\rm tot}|^2$ keeps nearly Lorentzian. This effect found for a purely quantum system in [31] is called the Lamb shift and in most part of works such as [32] is claimed to be a quantum effect also in MEF. Though the authors never dispute the existence of the classical analogues of this effect, only few authors such as those of [33] claim it to be a classical effect in MEF. The Lamb shift is accompanied by a decrease of $F^P_{\rm rad}(\omega)$ in the whole spectrum of the (still enhanced) fluorescence compared to $F^P_{\rm rad}(\omega_0)$ obtained for the optimal weak coupling. In the conventional MEF techniques $F^P_{\rm rad}$ in this regime does not exceed ten [32, 33].

Further increase of the coupling in our dimer results in the asymmetric splitting of the spectrum. Then a spectral minimum arises in the function $|d^{\rm tot}(\omega)|^2$ below ω_0 and a slightly asymmetric maximum holds above ω_0. This maximum is called the Fano resonance [34, 35] and the radiative Purcell factor at the corresponding frequency is nearly the same as the resonant gain in the regime of the Lamb shift [23].

The next level of the coupling corresponds to the regime when the fluorescence spectrum reshapes so that two nearly symmetric spectral maxima $\omega_+ > \omega_0$ and $\omega_- < \omega_0$ arise over the frequency axis. In this regime, the gain in the fluorescence decreases compared to the regimes of the Lamb shift and Fano resonance – the fluorescence power spectral density at the maxima is of the order of that corresponding to the single QE [30]. This is the aforementioned case of the Rabi splitting [17, 22, 23, 24, 30]. When the coupling grows further and exceeds a certain threshold the radiated power sharply decreases and becomes smaller than that of a single QE. In this regime, the NA is destructive for the fluorescence and constructive for the non-radiative power exchange in the dimer [36].

The Lamb shift, the Fano resonance, the birefringence in two strongly coupled circuits, and the wireless power transfer between two circuits – all these phenomena are well known in the classical electrodynamics, acoustics and mechanics. However, in the literature of nanophotonics a

point of view dominates that these effects in MEF cannot be described in a classical way, they have the quantum nature (see e.g. in [37]). Respectively, the majority of authors calculate the parameters of the corresponding structures using the semiclassical models based on quantum analogues of the Langevin equations of motion (see e.g. in [38]), on the Maxwell-Bloch equations (see e.g. in [39]), and on the Lindblad master equations (see e.g. in [40]). Well, the accuracy of the semi-classical models is not disputable, however, they are not very simple and rarely allow one to use the commercial software for calculating the system parameters. There are some authors who recognize that all these effects including the fluorescence quenching are classical effects and can be properly calculated without involving quantum mechanics. However, these authors consider the strong near-field coupling as the multipolar one (see e.g. in [41, 42]) that makes their classical model cumbersome and difficult.

2.2. Dipole model: closed-form solution

In work [43] a very simple classical dipole model was suggested that covers all these phenomena. If a source dipole (1) whose frequency spectrum in absence of the external field is $\mathbf{d}_1^{(0)}(\omega)$ couples to a passive dipole (2) whose polarizability is in the general case a tensor $\overline{\overline{\alpha}}_2(\omega)$, the dipole moment with the spectrum $\mathbf{d}_2(\omega)$ is induced in the passive dipole and additional dipole moment with the spectrum $\mathbf{d}_1^{(i)}(\omega)$ is induced in the active dipole due to its nonzero polarizability $\overline{\overline{\alpha}}_1(\omega)$. The resulting dipole moment of the active dipole is then $\mathbf{d}_1 = \mathbf{d}_1^{(0)} + \mathbf{d}_1^{(i)}$. Since $\mathbf{d}_1^{(i)}$ is proportional to $\mathbf{d}_2$, and $\mathbf{d}_2$ is induced by $\mathbf{d}_1^{(0)}$, we have for the total dipole moment of a dimer a relation $\mathbf{d}_{\rm tot} = \mathbf{d}_1^{(0)} + \mathbf{d}_1^{(i)} + \mathbf{d}_2 = \overline{\overline{F}}_d \cdot \mathbf{d}_1^{(0)}$, where tensor $\overline{\overline{F}}_d$ is as follows:

$$\overline{\overline{F}}_d = (\overline{\overline{I}} + \overline{\overline{\alpha}}_2 \cdot \overline{\overline{A}}_{12}) \cdot [\overline{\overline{I}} - (\overline{\overline{\alpha}}_1 \cdot \overline{\overline{A}}_{12}) \cdot (\overline{\overline{\alpha}}_2 \cdot \overline{\overline{A}}_{12}]^{-1}, \quad (2)$$

where $\overline{\overline{I}}$ is a unit tensor and $\overline{\overline{A}}_{12}$ is the tensor of dipole-dipole interaction relating the field $\mathbf{E}_{12}$ produced by dipole 1 (with the dipole moment $\mathbf{d}_1$) at the phase center of dipole 2: $\mathbf{E}_{12} \equiv \overline{\overline{A}}_{12} \cdot \mathbf{d}_1$. Due to reciprocity, the same coefficient expresses the field $\mathbf{E}_{21}$ produced by dipole 2 at the center of dipole1: $\mathbf{E}_{21} \equiv \overline{\overline{A}}_{12} \cdot \mathbf{d}_2$. In fact, in [43] a scalar analogue of (2) was derived. The vectorial form (2) is a straightforward generalization of the scalar formula [43]:

$$F_d = \frac{1 + \alpha_2 A_{12}}{1 - \alpha_1 \alpha_2 A_{12}^2}. \quad (3)$$

In the scalar case (when the dipoles $\mathbf{d}_{1,2}$ are directed along the same axis) and in vector case (different directions), we have for the radiative Purcell factor, respectively:

$$F_{\rm rad}^P = |F_d|^2, \quad F_{\rm rad}^P = {\rm Tr}\,[\overline{\overline{F}}_d^{\dagger} \cdot \overline{\overline{F}}_d], \quad (4)$$

where † denotes the Hermitian conjugation of a complex matrix.

The possibility to describe the electromagnetic coupling in the quantum dimer as a fully classical process is seen from the quantum theory of a two-level system [17]. This theory states that the fluorescence spectrum of a two-level system (a molecule or a quantum dot) in a uniform ambient is Lorentzian:

$$d_1^{(0)}(\omega) = \frac{d_{10}}{1 - \frac{\omega^2}{\omega_0^2} + j\frac{\omega\gamma_1}{\omega_0^2}}, \quad (5)$$

and the polarizability of the QE describing the induced dipole moment is also Lorentzian with the same resonance (ω_0) and damping (γ_1) frequencies [17]. In (5) d_{10} is the matrix element of the optical transition operator. Parameters d_{10}, ω_0 and γ_1 are, definitely, provided by the quantum theory. However, for the coupling problem these parameters are only the input data and their quantum origin does not contradict to our paradigm: that the electromagnetic interaction in the dimer is a classical dipole coupling.

For simplicity let us further restrict by the case of collinear dipoles. Then the polarizabilities α_1 and α_2 are scalars even for anisotropic QE and NA, when they are axial components of the corresponding polarizability tensors. We have

$$\alpha_{1,2} = \frac{\alpha_{10,20}}{1 - \frac{\omega^2}{\omega_0^2} + j\frac{\omega\gamma_{1,2}}{\omega_0^2}}, \quad (6)$$

where for the static polarizability α_{10} of our QE the quantum theory of [17] gives the formula $\alpha_{10} = 2d_{10}^2/\hbar\omega_0$.

Since, the NA is a classical resonant scatterer and the QE in its coupling with the NA behaves as a classical dipole antenna, formula (3) is applicable in all mentioned regimes from the regime of the strong Purcell effect to the fluorescence quenching. This assertion for checked in [43] by the comparison of the closed-form solution (3) with the results of the semi-classical model for a NA of type shown in Fig. 1(b). This NA was a dimer of Ag nanospheres and a QE was a spherical semiconductor nanocrystal (quantum dot) centered in the gap between the spheres. Gradually increasing the dipole moment d_{10} of the optical transition in the quantum dot, we gradually transit from the regime of the Purcell effect through the regime of the Lamb shift (when the fluorescence spectrum is still Lorentzian though the spectral maximum is shifted from ω_0 to ω_L) and the regime of the Fano resonance (a spectral hole in place of ω_L and a maximum slightly above ω_0)to the Rabi oscillations (when the spectral maxima at $\omega_\pm$ are close to one another). In [43] this evolution of the spectral shapes was shown in comparison with the known literature data.

Now, let us formulate the criteria of coupling. First of all, notice that in formula (3) there is no singularity. The value $\alpha_1\alpha_2 A_{12}^2$ is nearly positive only at low frequencies $\omega \ll \omega_0$ where this value is negligibly small compared to unity. In the resonance band of the NA it is complex in accordance to (6) and at higher frequencies A_{12} becomes essentially complex. However, $\alpha_1\alpha_2 A_{12}^2$ determines the level of coupling in the dimer. If it is much smaller than unity the coupling is insufficiently weak. When it is of the order

of unity, i.e.

$$|\alpha_2(\omega_0)A_{12}(\omega_0)| \gg 1, \quad |\alpha_1(\omega_0)A_{12}(\omega_0)| \ll 1.$$

the strong Purcell effect is observed. Then F_d in (3) reduces to $F_d \approx 1 + \alpha_2 A_{12}$ and we have for the resonant radiative Purcell factor

$$F^P_{\rm rad}(\omega_0) \approx |\alpha_2(\omega_0)A_{12}(\omega_0)|^2.$$

When we either increase the coupling coefficient A_{12} or the polarizability α_1 of the QE we increase the level of coupling. If $|\alpha_1(\omega)A_{12}(\omega)| \sim 1$ we have $|F_d| \approx |1/\alpha_1(\omega)A_{12}(\omega)| \sim 1$ because the term $|\alpha_2(\omega)A_{12}(\omega)| \gg 1$ in the fraction cancels out. It can be analytically shown that a Lorentzian frequency dispersion of α_1 and a weak dispersion of A_{12} in the resonance band together result in the birefringence of the resonance for $|F_d|^2$. Finally, if $|\alpha_1(\omega)A_{12}(\omega)|gg1$ we have $|F_d| \ll 1$ that points out to the fluorescence quenching because in the whole fluorescence spectrum we have $|d_{\rm tot}(\omega)| \ll |d_1^{(0)}(\omega)|$.

For calculation of F_d performed in [43] we needed the polarizability $\alpha_2(\omega)$ of the NA and the coupling coefficient $A_{12}(\omega)$ – the field produced by the NA at its phase center. In the numerical example of [43] both parameters were found from the classical full-wave simulation using the CST commercial software. To find $\alpha_2(\omega)$ the NA was excited by a Hertzian current source centered in the antenna gap. The dipole moment d_2 was found by a simple integration of the induced polarization in the NA and divided by the field produced by the Hertzian dipole at its center (which was also the center of the NA). The result turned out to be a pretty Lorentzian frequency function. In order to find $A_{12}(\omega)$ the NA in the CST simulator was impinged by an incident plane wave. The electric field E_{21} created by the dipole moment d_2 (induced in the NA by the incident wave) at its phase center was found as the total field minus the incident one and divided by d_2. These input parameters offered F_d found from (3) and the normalized spectra of the radiated power calculated for different values of d_{10}. These spectra nearly coincided in [43] with those previously found for this quantum dimer rigorously (in the literature). Thus, the applicability of the dipole model for the fluorescent dimer was confirmed.

2.3. Equivalent scheme of a dipole dimer

Any Lorentzian dipole radiator and scatterer can be presented as an effective LRC-circuit. In this paper, we will see how relevant is this presentation for a fluorescent dimer. The dipole moment d_2 of a NA (recall that we consider the case of the collinear polarization and vector notations are avoided) is related to the effective polarization current I_2 as $d_2 = I_2 l_2/j\omega$, where l_2 is the effective length of the NA. Our NA can be described by its effective impedance Z_2 referred to the phase center. Current I_2 being multiplied by Z_2 results in the electromotive force (EMF) $\mathcal{E}_2$ induced in the NA by the QE. This EMF is

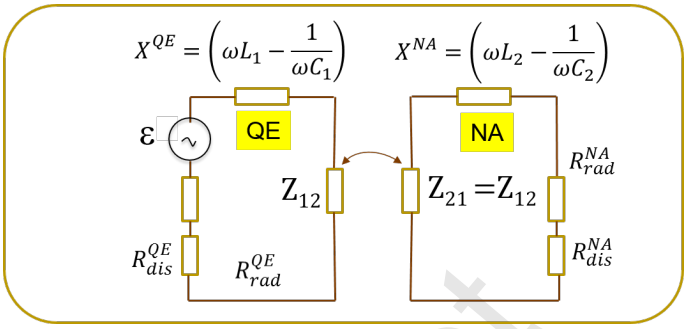

Figure 2: Equivalent scheme of a dimer with arbitrary coupling. Emissivity is modelled by a voltage generator.

equal to the product of the field E_{12} (produced by the QE at the phase center of the NA) by the effective length l_2 of the NA: $\mathcal{E}_2 = E_{21}l_2$. Then we have for its polarizability:

$$\alpha_2 = \frac{I_2 l_2}{j\omega E_{21}} = \frac{E_{21}l_2}{Z_2}\frac{l_2}{j\omega E_{21}} = \frac{l_2^2}{j\omega Z_2}. \qquad (7)$$

Here $Z_2 = R_2 + jX_2$, where $R_2 = R_{2\rm rad} + R_{2\rm dis}$ is the effective resistance of the scatterer and X_2 is its effective reactance comprising an inductive and capacitive components:

$$X_2 = \omega L_2 - \frac{1}{\omega C_2}, \quad L_2 C_2 = \frac{1}{\omega_0^2}. \qquad (8)$$

Substituting (8) into (7) allows us to yield α_2 to a Lorentzian form

$$\alpha_2(\omega) = \frac{l_2^2 C_2}{1 - \frac{\omega^2}{\omega_0^2} + j\frac{\omega\gamma_2}{\omega_0^2}}, \quad \gamma_2 = R_2 C_2 \omega_0^2, \qquad (9)$$

i.e. $\alpha_{20} = l_2^2 C_2$. A similar consideration was performed a century ago for a dipole antenna fed by an arbitrary time-harmonic source [45]. For an antenna whose sizes are small compared to the radiated wavelength it results in a series LRC-circuit with which the electromotive force (EMF) $\mathcal{E}$ and the output resistance R_g of the generator are connected in series. Interpreting our QE as a small transmitting antenna we come to the scheme depicted in Fig. 2. Here $R^{QE}_{\rm dis}$ and $R^{QE}_{\rm rad}$ are dissipative and radiative resistances of the QE, $R^{NA}_{\rm dis}$ and $R^{NA}_{\rm rad}$ are those of the NA, X^{QE} and X^{NA} are reactive parts of the of the impedances Z_1 and Z_2 (QE and NA, respectively), and Z_{12} is the mutual impedance of two circuits. If the coupling between our QE and NA is dipolar, we have for the EMF induced in the NA by the QE $\mathcal{E}_{12} = E_{12}l_2$. Therefore, Z_{12} defined as the ratio of the induced EMF $\mathcal{E}_{12}$ to the source current I_1 is equal to

$$Z_{12} = \frac{A_{12}d_1 l_2}{I_1} = \left(\frac{A_{12}I_1 l_1}{j\omega}\right)\frac{l_2}{I_1} = A_{12}\frac{l_1 l_2}{j\omega}, \qquad (10)$$

where l_1 is the effective antenna length of the QE.

2.4. Equivalent scheme of a weakly coupled dipole dimer

In Fig. 2, the EMF $\mathcal{E}$ describing the emission is connected in series to the generator resistance R_g. The theorem of an equivalent generator allows us to replace this

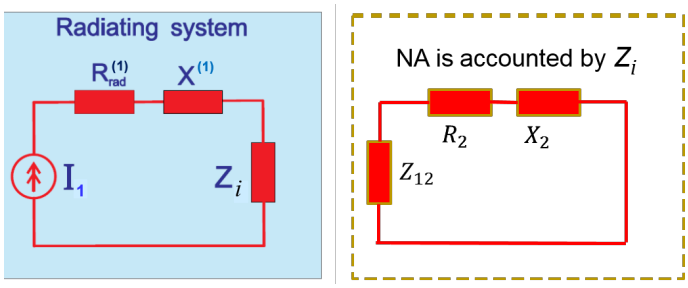

Figure 3: Equivalent scheme of a dimer with weak coupling where the emission is modelled by an ideal current generator. The passive circuit is included into the radiating system via the induced impedance.

effective voltage generator by the parallel connection of the effective current generator I_1 and its admittance Y_g. The scheme with the current generator is more relevant in the case of the weak coupling (strong Purcell effect). Really, the absence of the backward action means that the current I_1 is preserved: $d_1 = I_1 l_1/j\omega = d_1^{(0)} = I_1^{(0)} l_1/j\omega$. This is possible if and only if the current generator is ideal – $Y_g = 0$. Then the action of the NA is solely the change of the effective impedance to which this ideal current generator is connected. It can be taken into account by the inclusion of the circuit describing the NA into the circuit of the QE. For it, instead of the mutual impedance Z_{12} we load the active circuit by the induced impedance Z_i (sometimes, also called the shared impedance). In accordance to the method of induced EMFs [45] we have $Z_i = Z_{12} I_1/I_2$. The equivalent scheme of the radiating system in the case of the Purcell effect is shown in Fig. 3. In [19] the formula for Z_i in the case of the dipole coupling was derived:

$$Z_i = \frac{l_1^2 l_2^2 A_{12}^2}{\omega^2 Z_2}, \tag{11}$$

where $Z_2 = R_{dis}^{NA} + R_{rad}^{NA} + jX^{NA}$. In the case of the weak coupling $X_i = \mathrm{Im}(Z_i)$ vanishes at the frequency practically equal to $\omega_0 = 1/\sqrt{C_1 L_1} = 1/\sqrt{C_2 L_2}$ i.e. the resonance of the radiating system is almost not shifted [19]. The most important action of the NA in this regime is the increase of the Purcell factor in the fluorescence band. Since the NA is a much more efficient radiator than the QE we have $R_i \gg R_1$ and we have for the total Purcell factor

$$F_{\mathrm{tot}}^P(\omega) = 1 + \frac{R_i}{R_1} \gg 1. \tag{12}$$

In this formula, we can express $R_i = \mathrm{Re}(Z_i)$ through α_2 using (7). For the most part of fluorescent molecules the radiative decay rate strongly exceeds the dissipative one [46] and R_{dis}^{QE} can be neglected compared to R_{rad}^{QE}. The radiative resistance of a small dipole in free space (see e.g. in [45]) is as follows:

$$R_{\mathrm{rad}}^{QE} = \sqrt{\frac{\mu_0}{\varepsilon_0}} \frac{k^2 l_1^2}{6\pi}, \quad k \equiv \frac{\omega}{c}. \tag{13}$$

and we come to the relation (see also in [19]):

$$F_{\mathrm{tot}}^P(\omega) \equiv 1 + \frac{R_i}{R_1} = 1 + \frac{6\pi\varepsilon_0 c^3}{\omega^3} \mathrm{Re}[j\alpha_2(\omega) A_{12}^2]. \tag{14}$$

Formula (14) was validated in works [19, 44] by the comparison with the literature data for some particular NAs. This formula can be easily generalized to the case when our dimer is located in a dielectric medium with the refractive index n:

$$F_{\mathrm{tot}}^P = 1 - \frac{6\pi\varepsilon_0 n^2}{k^3} \mathrm{Im}(A_{12}^2 \alpha_2), \quad k \equiv \frac{\omega n}{c}. \tag{15}$$

2.5. Dissipative Purcell factor in the regime of the Purcell effect

Let us derive a relation between the radiative and dissipative Purcell for the case of the Purcell effect. This relation is missing in works [42, 43, 44]. The real part of Z_i comprises two components – a radiative one and a dissipative one, responsible for these two coefficients, respectively. It is not so easy to separate these two components of the resistance R_i. Therefore, to find the dissipative Purcell factor we subtract the radiative Purcell factor from the right-hand side of (15). The radiative Purcell factor in accordance to (3) equals to $F_{\mathrm{rad}}^P(\omega) \approx |1 + \alpha_2(\omega) A_{12}(\omega)|^2 = 1 + |A_{12}^2 \alpha_2|^2 + 2\mathrm{Re}(\alpha_2 A_{12}^*)$, where $*$ denotes the complex conjugation. Thus, we have

$$F_{\mathrm{dis}}^P = \frac{6\pi\varepsilon_0 n^2}{k^3} \mathrm{Im}(A_{12}^2 \alpha_2) - |A_{12}^2 \alpha_2|^2 + 2\mathrm{Re}(\alpha_2 A_{12}^*). \tag{16}$$

Let us restrict by the case when A_{12} is real. It corresponds to the capacitive coupling in the dimer and it is an adequate approximation for collinear polarization of both our dipoles [19]. It is instructive to present $\mathrm{Im}(\alpha_2)$ in (15) as

$$\mathrm{Im}(\alpha_2) = -|\alpha_2|^2 \left[\mathrm{Im}\left(\frac{1}{\alpha_2}\right)^{rad} + \mathrm{Im}\left(\frac{1}{\alpha_2}\right)^{dis} \right]. \tag{17}$$

The first term in the bracket of (17) is the radiating damping factor of a dipole scatterer [47]:

$$\mathrm{Im}\left(\frac{1}{\alpha_2}\right)^{rad} = \frac{k^3}{6\pi\varepsilon_0 n^2}.$$

Due to this term the second term in the right-hand side of (16) takes form $|\alpha_2|^2 A_{12}^2$ and cancels out with the third term. For the second term in the bracket of (17) we obtain from (9) the following relation:

$$\mathrm{Im}\left(\frac{1}{\alpha_2}\right)^{dis} = -\frac{\omega R_{dis}^{NA}}{l_2^2}.$$

Therefore Eq. (16) takes form

$$F_{\mathrm{dis}}^P = \frac{6\pi\varepsilon_0 n^2}{k^3} |\alpha_2| A_{12}^2 \frac{\omega R_{dis}^{NA}}{l_2^2} + 2A_{12}\mathrm{Re}(\alpha_2) \tag{18}$$

In the case of the strong Purcell effect we have for the resonance band $|\alpha_2 A_{12}|^2 \gg 2|\alpha_2 A_{12}| > 1$. Then neglecting the second term in the right-hand side of (18) we obtain

$$F^P_{\rm dis} \approx |\alpha_2|^2 A_{12}^2 \frac{R^{NA}_{\rm dis}}{R^{NA}_{\rm rad}}, \tag{19}$$

where we took into account that the radiative resistance of the NA is given by the generalization of (13) to the case of the host dielectric medium:

$$R^{NA}_{\rm rad} = \sqrt{\frac{\mu_0}{\varepsilon_0}} \frac{k^2 l_2^2}{6\pi n}, \quad k \equiv \frac{\omega n}{c}. \tag{20}$$

In the adopted approximation there is no need to keep unity in the expression $F^P_{\rm rad} \approx |\alpha_2|^2 A_{12}^2$, and the result (19) can be, finally, presented in the form:

$$F^P_{\rm dis} \approx F^P_{\rm rad} \frac{n R^{NA}_{\rm dis}}{R^{NA}_{\rm rad}}. \tag{21}$$

For a given ratio between the radiative and dissipative losses of a NA its dissipative Purcell factor grows along with the radiative one and is proportional to the refractive index of the medium. In the theory of wire antennas operating at radio frequencies the radiative and dissipative resistances of a short dipole are both directly proportional to n [48]. Formula (20) holds for any Hertzian dipole and shows that $R^{NA}_{\rm rad}$ is directly proportional to n. As to $R^{NA}_{\rm dis}$, its dependence on n may be different for different design solutions of a NA. Simple NAs such as plasmonic nanorods are quite similar to radio-frequency wire antennas, and the same direct proportionality of $R^{NA}_{\rm dis}$ to n holds for them [49]. Probably, the same refers to a bow-tie NA and to a core-shell plasmonic particle. For such NAs the factor n in (21) means that the radiation efficiency of a fluorescent dimer decreases when the refractive index of the host medium increases. This result seems to be important for MEF.

2.6. Equivalent scheme of a strongly coupled dimer

In the case of the strong coupling, the backward action of the NA to the QE is significant and the effective current $I_1 = j\omega d_1/l_1$ modifies compared to $j\omega d_1^{(0)}/l_1$. This means that the part of the current describing the emission flows though the internal admittance Y_g that cannot be neglected anymore. There is no difference to model the emission by such a non-ideal current generator with an unknown admittance or by a voltage generator with an unknown resistance R_g. In both cases to evaluate the generator effective resistance/admittance is problematic. Therefore, it is instructive to describe the emission by a single circuit element such as the negative resistance.

The idea to describe the fluorescence by a negative resistance was suggested in work [50]. If we admit this point, the LRC-circuit describing the QE comprises the resistor $R^{QE}_{\rm neg} < 0$. In Fig. 4 we show the corresponding equivalent scheme of our dimer. This scheme evidently makes sense

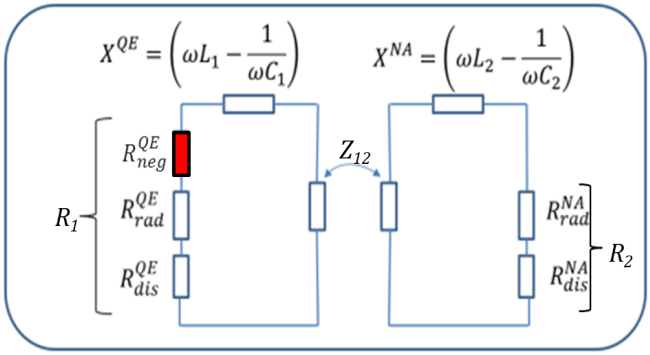

Figure 4: The circuit scheme of our dimer where the emissivity is modelled by the negative resistance $R^{QE}_{\rm neg}$.

only at the frequencies where the total impedance of the system vanishes. It does not allow us to find the fluorescence spectra and the emission spectra beyond the eigenmodes in this model are automatically neglected. However, the eigenmodes can be found properly.

Notice, that our circuit drastically differs from the circuit suggested in [50] which was evidently wrong and resulted in several non-physical conclusions mistakenly formulated by the authors. Probably, these incorrect conclusions blocked the further development of the idea to describe the emission by the negative resistor (that is applicable not only to the fluorescence). Below we develop this idea for two coupled circuits shown in Fig. 4. We do not include the circuit of the NA into the radiating system (though mathematically equivalent it would imply more algebra).

Eigenfrequencies of two coupled circuits described by their Kirchhoff equations

$$I_1 Z_1 + I_2 Z_{12} = 0,$$

$$I_1 Z_{12} + I_2 Z_2 = 0.$$

are found equating the determinant of this system to zero:

$$Z_1 Z_2 - Z_{12}^2 = 0. \tag{22}$$

After the substitution of (10) this equation takes form

$$-\omega^2 Z_1 Z_2 = (l_1 l_2 A_{12})^2 . \tag{23}$$

Substituting $Z_{1,2} = R_{1,2} + j\omega L_{1,2} + 1/j\omega C_{1,2}$ into Eq. (23) we easily obtain:

$$\left(1 - \frac{\omega^2}{\omega_0^2} + j\omega C_1 R_1\right)\left(1 - \frac{\omega^2}{\omega_0^2} + j\omega C_2 R_2\right) = \kappa^2. \tag{24}$$

Here it is denoted

$$\kappa = \sqrt{C_1 C_2} l_1 l_2 A_{12}. \tag{25}$$

This parameter is the coupling coefficient of our dimer. Equation (24) has spurious and physical solutions. Spurious ones are essentially complex, real ones are physically

sound. Obviously for real solutions R_1 should be negative so that to compensate the impact of the positive R_2 and positive $R_{\rm rad}^{QE} + R_{\rm dis}^{QE}$.

Within the resonance band we may neglect the frequency dispersion of the effective resistances and put $R_{1,2}(\omega) = R_{1,2}(\omega_0)$. Then in Eq. (23) all parameters are frequency independent, and this equation coincides with the dispersion equation of two inductively coupled circuits known in electronics or that of two elastically coupled oscillators known in mechanics. In fact, the coupling of two our circuits is not inductive, because the mutual impedance expressed by (10) for complex A_{12} has all possible components – inductive, capacitive and resistive. However, as it is explained in [43] in the case when ω_0 is the same for both QE and NA, their coupling coefficient κ can be expressed via the consolidated dipole-coupling coefficient A_{12}. However, if the resistive coupling is present, A_{12} and κ are complex values.

For simplicity assume again that A_{12} is a real and positive value that corresponds to the capacitive coupling. In this case the weak and intermediate coupling regimes (strong Purcell effect, Lamb shift and Fano resonance) can be observed for $\kappa < 0.01 - 0.02$ [43]. In the case when $\kappa > 0.01$ the coupling is strong and the solutions of Eq. (23) depend on the value $a \equiv \omega_0(C_1R_1 + C_2R_2)$. If $a \neq 0$ this equation explicitly comprises the imaginary term. Another important parameter is $\kappa_0^2 = C_1C_2|R_1|R_2\omega_0^2$.

2.7. Radiative Rabi oscillations and the resonant increase of dissipation

If $\kappa \gg 0.01$ it practically means that the coupling coefficient is much larger than $b \equiv C_1C_2|R_1|R_2\omega_0^2 \ll \kappa^2$. If κ is still smaller than κ_0 the physically sound solutions of Eq. (24) are possible only if $a = 0$ i.e. when $R_1 = -R_2C_2/C_1$. In this case (24) is biquadratic and its real solutions are as follows:

$$\frac{\omega_\pm}{\omega_0} \approx 1 \pm \kappa. \qquad (26)$$

Two frequencies $\omega_\pm$ describe the aforementioned Rabi oscillation and are called *Rabi frequencies*. The difference $\omega_+ - \omega_0 = \omega_0 - \omega_- = \omega_0\kappa$ is called the Rabi frequency shift and usually is denoted as Ω_R. The Rabi oscillation comprises two Rabi frequencies with the nearly equal amplitudes and physically represents the beating. This beating oscillation corresponds to the power exchange between two our circuits. One half-period of the beating the energy transfers from the QE to the NA and in the other half-period returns back. In the present case, when the coupling is not overcritical, the Rabi oscillations are radiative.

If we calculate $R_i = \mathrm{Re}(Z_i)$ given by formula (11) for this case we will see that the absolute value of $R_i(\omega_\pm)$ is not as large as it was in the case of the Purcell effect. Moreover, in this case the approximation we adopted deriving (21) are not valid anymore, and the dissipative Purcell factor may prevail on the radiative one even in free space ($n = 1$). Though in the present case the dipole moment d_1 changes due to the presence of the NA, our definition of the radiative Purcell factor (4) keeps relevant for description of the fluorescence spectrum. Really, the radiated power of our dimer in this definition is normalized to the power radiated by a single QE. Therefore, in the regime of Rabi oscillation $F_{\rm rad}^P = |F_d|^2$ still properly describes the impact of the NA for the fluorescence.

Moreover, the total Purcell factor given by formula (14) also keeps relevant for the strong-coupling regime. In this formula, the total power loss (dissipative and radiative) of the quantum dimer is normalized to the loss of the single QE. Therefore, the comparison of $F_{\rm tot}^P$ and $F_{\rm rad}^P$ allows us to share out the radiative and the dissipative components in the induced resistance R_i.

Let us show how it works for the nanostructure numerically analyzed in work [43] and partially described above. That NA was a plasmonic dimer consisting of two Ag nanospheres of diameter 14 nm separated by the gap 8 nm in free space. This NA resonated at $\lambda_0 = 2\pi c/\omega_0 =$450 nm. Aforementioned CST simulations were done so that to find both α_2 and the coupling coefficient A_{12} referred to the phase center of the dimer. An emitter was a quantum dot centered in the gap of the plasmonic dimer i.e. the centers of the NA and QE coincided. The coupling was gradually increased by the increase of the quantum dot polarizability from zero to $d_{10} = 1.12 \cdot 10^{-28}\, C{\cdot}$m (or 35 D in debyes). For this case, the effective cross section of *radiative* emission calculated in [43] manifested the symmetric Rabi oscillations without a gain compared to the single QE.

Let us compare $F_{\rm tot}^P$ and $F_{\rm rad}^P$ for this case. The CST simulations have shown that the approximation of real A_{12} and κ is not valid for the whole spectrum. In Fig. 5 (left panel) we see both real and imaginary parts of A_{12} which resulted together with other retreived parameters in the emission spectra presented in [43]. The imaginary part of A_{12} is not negligible at λ_0, but at the Rabi wavelengths $\lambda_+ = 2\pi c/\omega_+ \approx$435 nm and $\lambda_- = 2\pi c/\omega_- \approx$465 nm the approximation of the real coupling coefficient is adequate that makes the example discussed in [43] compatible with the present simplistic analysis.

In Fig. 5 (right panel) we see $F_{\rm rad}^P$ calculated using formulas (3) and (4) in comparison with $F_{\rm tot}^P$ calculated using formula (14). The total Purcell factor strongly dominates over the radiative one over the whole resonance range. In other words, the NA effectively inserts a resonant dissipation into the QE and this resonance is split onto two Rabi frequencies. Here, R_i can be identified with $R_i^{\rm dis}$, the radiative component of the induced impedance is very small. In Fig. 5 we also see that $F_{\rm rad}^P$ nearly attains unity at the Rabi wavelengths. This means that the Rabi oscillations in spite of a very high dissipation keep radiative and the emission level is not altered by the NA. In this regime, the impact of the NA is twofold: it splits the fluorescence frequency and drastically increases the absorption of the pumping radiation.

Let us stress that if $\kappa < \kappa_0$ the assumption that $a \neq 0$

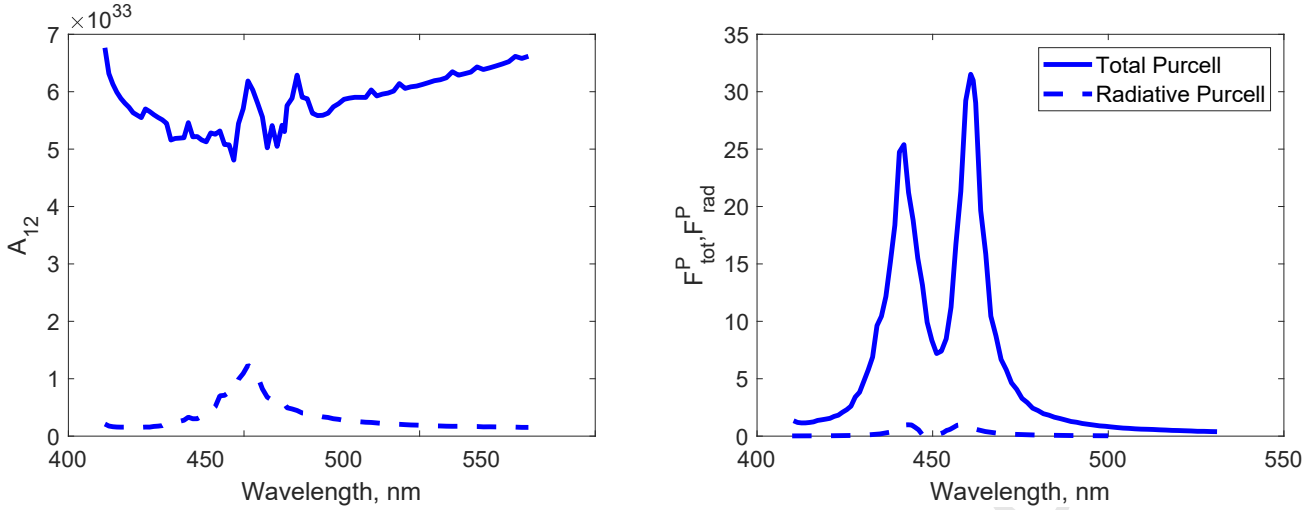

Figure 5: Left: dipole coupling coefficient for a QE and a NA from work [43] retrieved from the classical simulations. Solid curve – $\mathrm{Re}(A_{12})$, dashed curve – $\mathrm{Im}(A_{12})$. Right: total (solid) and radiative (dashed) Purcell factors calculated in the fluorescence spectrum for the case $d_{10} = 35$ D.

does not grant us physically sound solutions. Only the condition $a = 0$ corresponds to physically sound Rabi oscillations. The radiative and dissipative losses in this regime are exactly compensated by the negative resistance.

2.8. Non-radiative Rabi oscillations

Now, let us consider the regime of the overcritical coupling when

$$\kappa^2 > \kappa_0^2 = C_1 C_2 |R_1| R_2 \omega_0^2. \tag{27}$$

This case was not considered in work [43] because the only goal of that numerical study was validation of the theory. The emission spectra obtained using the quantum model for a so high coupling as given by (27) were absent in the literature. Moreover, in [43] the concept of the negative resistor was not concerned.

However, all we need to find the threshold value κ_0 is A_{12} and α_2 which do not depend on d_{10} and were found preparing the article [43] and α_1 that can be easily calculated for given d_{10} using (6). Here we use the knowledge of ω_0 and identify γ_1 with the radiative damping (see above):

$$\gamma_1 = \sqrt{\frac{\mu_0}{\varepsilon_0}}\frac{\alpha_{10}\omega_0^2 k^2}{6\pi}, \quad \alpha_{10} = \frac{2d_{10}^2}{\hbar\omega_0}.$$

The increase of d_{10} is the same as the increase of κ. Really, the expression in the right-hand side of (25) comprises the factor $\sqrt{C_1 l_1^2}$ which is equal to $\sqrt{\alpha_{10}} = d_{10}\sqrt{2/\hbar\omega_0}$. If we continue to gradually increase d_{10} above the value of 35 D we come to the regime when the radiative Purcell factor $|F_d|^2$ given by (3) vanishes in the whole spectrum. It occurs when $d_{10} = (2.5 - 3) \cdot 10^{-28}\, C{\cdot}\mathrm{m}$. Meanwhile, the curve $F^P_{\mathrm{tot}}(\lambda)$ keeps practically the same as in Fig. 5.

This regime is nothing but the fluorescence quenching. Our dipole model allows us to find its threshold for the dipole moment d_{10} of the optical transition in a single quantum dot. After this threshold (nearly 80 D) the Rabi oscillations are non-radiative. Solutions (26) imply the necessary condition $a = 0$ of this regime that determines $R_1 = -R_2 C_2/C_1$ and the value of the negative resistor R^{QE}_{neg} describing the emission at the Rabi frequencies can be expressed through the known parameters of the single QE (R^{QE}_{rad}, R^{QE}_{dis}, C_1) and the single NA (R^{NA}_{rad}, R^{NA}_{dis}, C_2).

2.9. Spaser

Now, let us assume that the coupling is overcritical and simultaneously $a < 0$. At a first glance, this assumption makes the physically sound solutions impossible since in our Eq. (24) an imaginary term appears. However, in the theory of instability the almost real complex frequencies make sense. The case when $\kappa^2 = \kappa_0^2(1 + \xi)$, with small positive ξ ($\xi \ll |a|$) grants to our dispersion equation an almost real root with a very small *positive* imaginary part:

$$\left(\frac{\omega_s}{\omega_0}\right)^2 \approx 1 - j\frac{\kappa^2 - \kappa_0^2}{2a}. \tag{28}$$

Solution (28) has a physical meaning – it is an instable eigenmode whose positive imaginary part is an increment. The increment describes the broken equilibrium at the initial stage of the accumulation of the electromagnetic energy in the dimer. The energy accumulates in the form of growing localized surface plasmon in the NA at the frequency of its individual resonance.

In fact, in the case when $a < 0$ Eq. (24) has three physically sound complex solutions. One of them is ω_s and two other solutions are decaying Rabi oscillations $\mathrm{Re}(\omega) \approx \omega_+$ and $\mathrm{Re}(\omega) \approx \omega_-$ with small negative imaginary parts.

The regime is hardly realizable with a single quantum source coupled to a nanoantenna. Most probably, any quantum dot (moreover, any molecule) converting the

pumping radiation into non-radiative emission cannot perform both functionalities: compensation of the drastically increasing dissipative losses (see above) and growth of the plasmon in the NA. To achieve the generation our NA should be coupled to $N \gg 1$ simultaneously fluorescent emitters. Then the negative resistance of a single QE multiplies by N. This multiplication implies that the emitters are not mutually coherent. If our N emitters oscillated coherently, their negative resistors should have been multiplied by N^2. However, such the coherent emission also called superemission may occur only on the next stage of the oscillation, that we do not concern here. Our linear model is applicable only to the initial stage when a non-coherent oscillation in the quenched fluorescent dimer starts to grow. When the coherent emission arises and the effective current in the NA becomes stimulated our circuit model as that referring to Lorentzian radiators/scatterers loses the validity. Basically, below we discuss only a prerequisite of a spaser assuming that the pumping is non-coherent. Coherent pumping cannot invert the population of the localized plasmon states – in the terms of the present paper it cannot grant the negative resistance to the QE.

For a spaser formed by a NA strongly coupled to N polarized QEs the first generation condition $a < 0$ can be rewritten as follows:

$$R_1 \equiv R_{\rm neg}^{QE} + R_{\rm rad}^{QE} + R_{\rm dis}^{QE} < -\frac{C_2 R_2}{N C_1}, \qquad (29)$$

where $R_{\rm neg,rad,dis}^{QE}$ correspond to a single QE. In fact, in order to overcompensate all losses in the dimer the negative resistor of a QE should be much larger than $R_{\rm rad}^{QE} + R_{\rm dis}^{QE}$ and in Eq. (29) we may neglect $R_{\rm rad,dis}^{QE}$. Then this equation takes form

$$R_1 \approx R_{\rm neg}^{QE} < -\frac{C_2 R_2}{N C_1}. \qquad (30)$$

Condition (30) is necessary but not enough for generation. The second condition is that of the overcritical coupling – inequality (27). In fact, there is also the third condition – that the amplitude of the egenmode (28) is nonzero whereas the amplitudes of the decaying Rabi oscillations are zeros. However, our phenomenological model does not reveal when it is so and this condition is not expressed by a formula. The quantum theory of the spaser shows that the generation may arise if the pumping is not coherent. In the case of the coherent pumping at frequency ω_0 there is no inverse population of the plasmon quantum states (in the quantized NA). In our model, the inverse population corresponds to $a < 0$. The regime with $a = 0$ correspond to the equilibrium in the non-radiative Rabi exchange of power between the QE and the NA. If the ground state is more populated ($a > 0$), the concept of the negative resistor is not relevant and we have to model the steady emission by a generator. This is the case of the weak coupling.

2.10. Negative resistor of a spaser

Formulas (27) and (30) are circuit analogues of two conditions known in the quantum theory of a spaser (see e.g. in [36]):

$$\Omega_R^2 > \gamma_1\gamma_2, \quad \tau_1\tau_2\Omega_R^2 N D_p > 1. \qquad (31)$$

Here $\Omega_R \equiv (\omega_+ - \omega_-)/2$ is the Rabi frequency shift, $\tau_1 = 1/\gamma_1^{\rm rad}$ is the radiative lifetime of the QE, $\tau_2 = 1/\gamma_2$ is the lifetime of the localized plasmon in the NA, and D_p is the eigenvalue of the *pumping efficiency operator*. In our model $\tau_1 = 1/\omega_0^2 R_{\rm rad}^{QE} C_1$.

Since $\Omega_R = \omega_0\kappa$ inequalities (31) are equivalent in our notations to following conditions:

$$\frac{\omega_0^2\kappa^2}{\gamma_1\gamma_2} > 1, \quad D_p > \frac{\gamma_1^{\rm rad}\gamma_2}{N\omega_0^2\kappa^2} = \frac{\omega_0^2 C_1 C_2 R_{\rm rad}^{QE} R_2}{N(l_1 l_2 A_{12})^2}. \qquad (32)$$

First inequality in (32) is nothing else but our condition of the overcritical coupling (27). It does not give us anything new and can be considered only as a check. Second inequality in (32) means that the power sufficient for generation is transferred to the dimer from the pumping source. This condition is what we need to determine our negative resistor.

So, we assume that our condition (30) is equivalent to the second inequality in (32). Substituting formula (13) for $R_{\rm rad}^{QE}$ we deduce the last inequality to the form

$$D_p \frac{A_{12}^2 l_2^2 6\pi}{\omega_0^4 \mu_0^2} > \frac{R_2}{N}. \qquad (33)$$

Our circuit model requires the same in the form

$$|R_{\rm neg}^{QE}|\frac{C_2}{C_1} > \frac{R_2}{N}. \qquad (34)$$

There is no physical contradictions between formulas (33) and (34) and they are equivalent if we impose for our negative resistor

$$|R_{\rm neg}^{QE}| = D_p \frac{6\pi l_2^2 A_{12}^2 C_1}{\mu_0^2 \omega_0^4 C_2}. \qquad (35)$$

So, the negative resistor of the spaser presented in the form of an equivalent circuit is found from the output data of the quantum model. Formula (35) is physically sound. Really, the higher is the pumping efficiency D_p, the higher is the emission (radiative or non-radiative, does not matter). Therefore, the negative resistor describing it should grow along with D_p. Next, the higher is the product $A_{12} l_2$ the higher is the power transfer from the QE into the NA. Higher power transfer obviously means higher emission. Therefore, the negative resistor should grow also along with $A_{12} l_2$. When our negative resistor is large enough and the coupling is overcritical, the pumping efficiency is sufficient for the generation. It is not so easy to explain the effective capacitance in the denominator of (35). However, in any case the two models of the spaser – the classical and the quantum ones – are not contradictory.

3. Conclusions

In the present paper, a classical dipole model of the general phenomenon called metal-enhanced fluorescence was developed. The initial basics of this approach were outlined in [43] and implemented for a particular case in [44]. However, several basic questions remained unanswered in these papers. First, for the case of the weak coupling the issue of the dissipative (non-radiative) Purcell factor was not clarified. Second, for the case of the strong coupling the generator describing the emission was not sufficiently explained. In this case the effective internal resistance of the generator mimicking the emission cannot be neglected, but the dipole model does not allow us to find both effective current (or electromotive force) and effective resistance of the generator. Therefore, it turned out to be instructive to describe the emission by a single element such as the negative resistor.

With this update, the previously developed concept allows us to analyze the regime of Rabi oscillations and to specify the cases of radiative and non-radiative ones. An increment of the emission is obtained for the case when the nanoantenna and N quantum sources are properly coupled and sufficiently pumped by a non-coherent radiation. In this scenario, we transit from the case of MEF to the case of the so-called spaser. In what concerns spasers, our classical model does not compete with the quantum model. It is only a simple illustration to the linear stage of the generation when the interplay between the coherent and non-coherent types of emission has not yet started. Being very simple and illustrative, our model can be instructive as an introduction for those researchers who do not wish to engage substantially with quantum physics but are eager to get an insight into this topic.

Finally, it is worth to notice that the present model of the dipole coupling, perhaps also accompanied by circuit schemes, can be applicable not only to the fluorescence. In surface-enhanced Raman scattering the Purcell effect has the key importance (see e.g. in [51]) and it is also observed in chemical luminescence when the plasmonic nanoparticles are added to the luminol [52]. Perhaps, a number of phenomena mentioned with respect to MEF still await to be unveiled and analyzed with respect to chemiluminescence.

Acknowledgement

The author is grateful to Alexey P. Vinogradov for a fruitful discussion.

References

[1] H. Sahoo, Fluorescent labeling techniques in biomolecules: a flashback, *RSC Advances* **2**, 7017–7029 (2012)

[2] M. Cox, D.R. Nelson, and A.L. Lehninger, *Lehninger's principles of biochemistry*, W.H. Freeman Publishers, San Francisco, CA (2008)

[3] A. Stallmach, C. Schmidt, A. Watson, and R. Kiesslich, An unmet medical need: advances in endoscopic imaging of colorectal neoplasia, *J. Biophoton.* **4**, 482–489 (2011)

[4] M. Kang, P. Xenopoulos, S. Munoz-Descalzo, X. Lou, and A.-K. Hadjantonakis, Live imaging, identifying, and tracking single cells in complex populations In Vivo and Ex Vivo, *Methods Mol. Biol.* **1052**, 109-123 (2013)

[5] T. Fujii, M. Kamiya, and Y. Urano, In vivo imaging of intraperitoneally disseminated tumors in model mice by using activatable fluorescent small-molecular probes for activity of cathepsins, *Bioconjug. Chem.* **25**, 1838–1846 (2014)

[6] S. Sensam, C.L. Zavaleta, E. Segal, S. Rogalla, W. Lee, S.S. Gambhir, M. Bogyo, and C.H. Contag, A clinical wide-field fluorescence endoscopic device for molecular imaging demonstrating cathepsin protease activity in colon cancer, *Mol. Imag. Biol.* **18**, 820-829 (2016)

[7] F. Tam, G.P. Goodrich, B.R. Johnason, and N.J. Halas, Plasmonic enhancement of molecular fluorescence, *NanoLett.* **7**, 496-501 (2007)

[8] J.R. Lakowicz, K. Ray, M. Chowdhury, H. Szmacinski, Y. Fu, J. Zhang, and K. Nowaczyk, Plasmon-controlled florescence: a new paradigm in fluorescence spectroscopy, *Analyst* **133**, 1308–1346 (2008)

[9] M. Bauch, K. Toma, Q. Zhang, and J. Dostalek, Plasmon-enhanced fluorescence biosensors: a review, *Plasmonics* **9**, 781-799 (2014)

[10] S.A. Camacho, P.H.B. Aoki, P. Albella, O.N. Oliveira, C.J.L. Constantino, and R.F. Aroca, Increasing the enhancement factor in plasmon-enhanced fluorescence with shell-isolated nanoparticles, *J. Phys. Chem. C* **120**, 20530-20535 (2015)

[11] Y. Pang, Z. Rong, R. Xiao, and S. Wang, Turn on and label-free core-shell Ag-SiO2 nanoparticles-based metal-enhanced fluorescent (MEF) aptasensor for Hg2+, *Sci. Rep.* **5**, 9451 (2015)

[12] T.D. Corrigan, S.-H. Guo, R. J. Phaneuf and H. Szmacinski, Enhanced fluorescence from periodic arrays of silver nanoparticles, *Journal of Fluorescence* **15**, 777-790 (2005)

[13] O. Tovmachenko, C. Graf, D.J. van den Heuvel, A. van Blaaderen, and H.C. Gerritsen, Fluorescence enhancement by metal-core/silica-shell nanoparticles, *Adv. Mat.* **18**, 91-95 (2006)

[14] D. Gontero, A. V. Veglia, A. G. Bracamonte and D. Boudreau, Synthesis of ultraluminescent gold core–shell nanoparticles as nanoimaging platforms for biosensing applications based on metal-enhanced fluorescence, *RSC Advances* **7**, 10252–10258 (2017)

[15] *Gold Nanoparticles For Physics, Chemistry And Biology* (Second Edition), C. Louis and O. Pluchery, Editors, World Scientific Publishing Europe, London (2017), p. 404

[16] E.M. Purcell, Spontaneous emission probabilities at radio frequencies, *Phys. Rev.* **69**, 681-687 (1946)

[17] L. Novotny and B. Hecht, *Principles of Nano-Optics*, Cambridge University Press, Cambridge, UK (2006)

[18] Q. Gu, B. Slutsky, F. Vallini, J.S. Smalley, M.P. Nezhad, N.C. Fratechi, and Y. Fainman, Purcell effect in sub-wavelength semiconductor lasers, *Optics Express* **21**, 15603-15617 (2013)

[19] A.E. Krasnok, A.P. Slobozhanyuk, C.R. Simovski, S.A. Tretyakov, A.N. Poddubny, A.E. Miroshnichenko, Y.S. Kivshar, and P.A. Belov, An antenna model for the Purcell effect, *Sci. Rep.* **5**, 12956-12978 (2015)

[20] A. Kinkhabwala, Z. Yu, S. Fan, Y. Avlasevich, K. Müllen and W.E. Moerner, Large single-molecule fluorescence enhancements produced by a bowtie nanoantenna, *Nat. Photon.* **2**, 654-657 (2009)

[21] T.H. Taminiau, F.D. Stefani, F.B. Segernik and N.F. van Hulst, Optical antenas direct single molecule emission, *Nat. Photon.* **2**, 234-237 (2008)

[22] G. Khitrova, H. M. Gibbs, M. Kira, S.W. Koch, and A. Scherer, Vacuum Rabi splitting in semiconductors, *Nature Phys.* **2**, 81-86 (2006)

[23] P. Bharadwaj and L. Novotny, Spectral dependence of single molecule fluorescence enhancement, *Opt. Express* **15**, 14266-14271 (2007)

[24] S. Savasta, R. Saija, A. Ridolfo, O. Di-Stefano, P. Denti, and F. Borghese, Nanopolaritons: vacuum Rabi splitting with a single quantum dot in the center of a dimer nanoantenna, *ACS Nano* **4**, 6369–6376 (2010)

[25] P. Anger, P. Bharadwaj, and L. Novotny, Enhancement and quenching of single-molecule fluorescence, *Phys. Rev. Lett.* **96**, 113002 (2006)

[26] P.K. Jain and M.A. El-Sayed, Plasmonic coupling in noble metal nanostructures, *Chem. Phys. Lett.* **487**, 153-164 (2010)

[27] A. Delga, J. Feist, J. Bravo-Abad, F.J. Garcia-Vidal, Quantum emitters near a metal nanoparticle: strong coupling and quenching, *Phys. Rev. Lett.* **112**, 253601 (2014)

[28] D.J. Bergman and M.I. Stockman, Surface plasmon amplification by stimulated emission of radiation: quantum generation of coherent surface plasmons in nanosystems, *Phys. Rev. Lett.* **90**, 027402 (2003)

[29] M.I. Stockman, The spaser as a nanoscale quantum generator and ultrafast amplifier, *J. Optics* **12**, 024004 (2008)

[30] M.I. Stockman, Spasers explained, *Nat. Phot.* **2**, 327-330 (2008)

[31] W.E. Lamb, Jr. and R.C. Retherford, Fine structure of the hydrogen atom by a microwave method, *Phys. Rev.* **72**, 241-244 (1947)

[32] Q. Sun, M. Al-Amri, A. Kamli, and M.S. Zubairy, Lamb shift due to surface plasmon polariton modes, *Phys. Rev. A* **77**, 062501 (2010)

[33] M. Rybin, S. Mingaleev, M. Limonov, and Y. Kivshar, Purcell effect and Lamb shift as interference phenomena, *Sci. Rep.* **6**, 20599 (2016)

[34] U. Fano, Effects of configuration interaction on intensities and phase shifts, *Phys. Rev.* **124**, 1866–1878 (1961)

[35] B. Luk'yanchuk1, N.I. Zheludev, S.A. Maier, N.J. Halas, P. Nordlander, H. Giessen and C.T. Chong, The Fano resonance in plasmonic nanostructures and metamaterials, *Nat. Mat.* **9**, 707-715 (2010)

[36] E.S. Andrianov, A.A. Pukhov, A.V. Dorofeenko, A.P. Vinogradov, and A. A. Lisyansky, Rabi oscillations in spasers during non-radiative plasmon excitation, *Phys Rev. B* **85**, 035409 (2012)

[37] E. Dulkeith, A.C. Morteani, T. Niedereichholz, T.A. Klar, J. Feldmann, S.A. Levi, F.C. van Veggel, D.N. Reinhoudt, M. Möller, and D.I. Gittins, Fluorescence quenching of dye molecules near gold nanoparticles: radiative and nonradiative effects, *Phys. Rev. Lett.* **89**, 203002 (2002)

[38] S. Rudin and T.L. Reinecke, Oscillator model for vacuum Rabi splitting in microcavities, *Phys Rev. B* **59**, 10227-10233 (1999)

[39] X.-W. Chen, V. Sandoghdar, and M. Agio, Coherent interaction of light with a metallic structure coupled to a single quantum emitter: from superabsorption to cloaking, *Phys. Rev. Lett.* **110**, 153605 (2013)

[40] E.D. Chubchev, E.S. Andrianov, A.A. Pukhov, A.P. Vinogradov, and A.A. Lisyansky, On correctness of the two-level model for description of active medium in quantum plasmonics, *J. Phys. B* **50**, 175401 (2017)

[41] G. Sun, J. B. Khurgin, and C. C. Yang, Impact of high-order surface Plasmon modes of metal nanoparticles on enhancement of optical emission, *Appl. Phys. Lett.* **95**, 171103 (2009)

[42] G. Sun and J. B. Khurgin, Origin of giant difference between fluorescence, resonance, and nonresonance Raman scattering enhancement by surface plasmons, *Phys. Rev. A* **85**, 063410 (2012)

[43] C. Simovski, Circuit model of plasmon-enhanced fluorescence, *Photonics* **2**, 568-593 (2015)

[44] C. Simovski, Point dipole model for metal-enhanced fluorescence, *Opt. Lett.*, in print. Available online. Doc. ID 355756

[45] S.A. Schelkunoff and H.T. Friis, *Antennas: Theory and Practice*, Wiley, New York–London (1952)

[46] B. Valeur and M.N. Berberan-Santos, *Molecular Fluorescence: Principles and Applications*, 2d Ed., Wiley-VCH, New York (2012)

[47] J.D. Jackson, *Classical Electrodynamics*, Wiley, New York, 3nd ed. (1999), pp. 748. See also in A. Wokaun, J.P. Gordon, and P.F. Liao, Radiation damping in Surface-Enhanced Raman Scattering, *Phys. Rev. lett.* **48**, 1574-1577 (1982)

[48] R.W.P. King, G.S. Smith, M Owens, and T.T. Wu, *Antennas in Matter*, The MIT Press, Gambridge, MA (1981)

[49] A. Alú and N. Engheta, Input impedance, nanocircuit loading, and radiation tuning of optical nanoantennas, *Phys. Rev. Lett.* **101**, 043901 (2008)

[50] J.-J. Greffet, M. Laroche, and F. Marquier, *Impedance of a nanoantenna and a single quantum emitter*, *Phys. Rev. Lett.* **105**, 117701 (2010)

[51] S.I. Maslovski and C.R. Simovski, Purcell factor and local intensity enhancement in surface-enhanced Raman scattering, *Nanophotonics*, https://doi.org/10.1515/nanoph-2018-0190

[52] A. Karabchevsky, A. Mosayyebi, and A.V. Kavokin, Tuning the chemiluminescence of a luminol flow using plasmonic nanoparticles, *Light: Science and Applications* **5**, e16164 (2016)